

Sorbent extraction behavior of a nonionic surfactant, Triton X-100, onto commercial charcoal from low level radioactive waste

Mostafa M. Hamed

Received: 22 February 2014 / Published online: 8 June 2014
© Akadémiai Kiadó, Budapest, Hungary 2014

Abstract In nuclear power plants and nuclear laboratories, laundry wastewater is generated from decontaminating polluted instruments, worker's clothes and taking shower after work. Laundry wastewater contains radionuclides and surfactants. The surfactants included in laundry wastewater affect the extraction of radionuclides. Therefore, surfactants should be removed before extraction of radionuclides. The objective of the present work is to assess the ability of commercial charcoal for the removal of nonionic surfactants, where, commercial charcoal is a commonly available adsorbent for treatment. Charcoal was characterized using different analytical techniques. The isotherm models and thermodynamic parameters were evaluated. Charcoal was applied to the removal of surfactant from liquid radioactive waste. The data obtained can be used for designing a plant for treatment of surfactant rich water and wastewater economically.

Keywords Adsorption · Nonionic surfactant · Triton X-100 · Liquid radioactive waste

Introduction

Surface active agents (surfactants) are in a widespread use throughout the world. Million tons of surfactants are produced annually [1]. Three concepts need to be considered in order to be able to understand the mechanisms of work in surfactant solutions such as solubility, adsorption on a

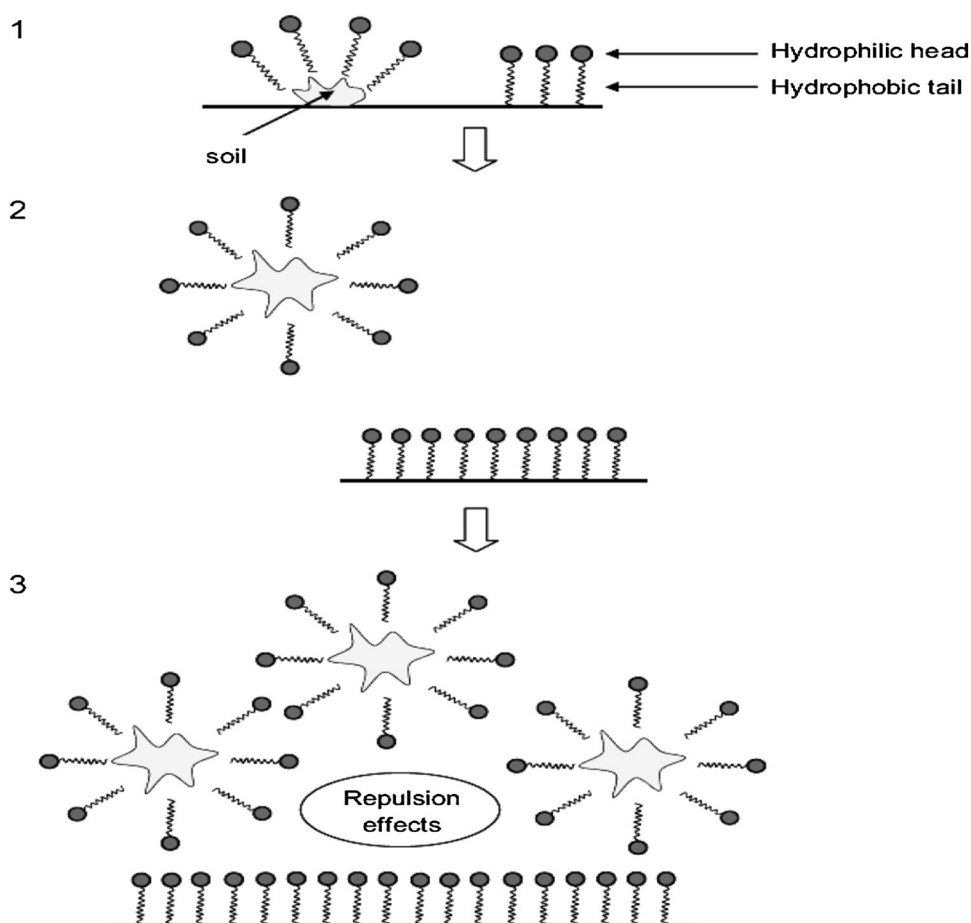
surface and the formation of micelles. The adsorption property is that provides the surface active effects of foaming, wetting, emulsification, dispersion of solids and detergency. The functional effects of emulsification and detergency are also accompanied by the formation of micelles. Surfactants reduce surface tension in water and other liquids through the accumulation of oriented molecules at the interface. This property derives from their amphiphilic structure which includes a hydrophilic head and a hydrophobic tail within the same molecule. The cleaning and dispersant effects of surfactants are due to the aforementioned interfacial activity and it is shown in Fig. 1. Surfactants are widely used for solubilization/mobilization purposes in a wide range of uses in technical applications such as agrochemicals, the metal and mining industry, polymers, microelectronic, paper industries, etc. [1]. Understanding the adsorption mechanism of surfactant molecules at the solid–liquid interface is an important way toward modeling industrial processes which use surfactants on a large scale [1, 2].

Such extensive applications of surfactants have produced environmental pollution and have raised problems in wastewater treatment plants [1, 3]. The experimental data have shown that surfactants can kill microorganisms at very low concentrations (1–5 mg/L) and harm them at even lower concentrations (0.5 mg/L). In addition, surfactants can produce foams, which are a significant problem in liquid waste treatment. Therefore, the removal of the surfactants from wastewater is important in reducing their environmental impact [3].

The generation of liquid radioactive wastes varies from country to country depending on the applications and type of activity associated with nuclear and radioactive material utilization in that country. These wastes can affect all forms of life, so their safe removal and treatment has

M. M. Hamed (✉)
Analytical Chemistry and Environmental Control Department,
Hot Laboratories and Waste Management Center, Atomic
Energy Authority, P.O. Box 13759 Cairo, Egypt
e-mail: mmhm8@yahoo.com

Fig. 1 Mechanism of dust or waste removal: (1) adhesion; (2) separation and (3) repulsion [1]



received considerable attention worldwide [4–6]. Treatment of liquid radioactive waste quite often involves the application of several steps to meet the requirements both for the release of decontaminated effluents into the environment and the conditioning of waste concentrates for disposal [5–7].

Large amounts of hot shower and laundry waste water, which include organic compounds such as residual cleaner, complexing reagents and low level radioactive materials, are generated in nuclear laboratories and nuclear power plants. There is a need to develop technology for its simple, cheap and fast purification treatment. The treatment system usually consists of the following two processes. The first process is removal of organic compounds from the waste water, the major one being surfactants. The second process is removal of such precipitants as iron oxides which include radioactive species [6, 8, 9]. A particular problem is posed by low level radioactive waste (LRW) from special laundries of nuclear laboratories and nuclear power plants, whose processing is complicated by their high content of surfactants and other components of detergents used. The presence of surfactants in radioactive waste affects the extraction and removal of Co^{2+} , Sr^{2+} and Cs^+ [5].

Various methods have been suggested for removal of these compounds such as preliminary oxidation with potassium permanganate or Fenton's reagent, ozonation, membrane purification, electrocoagulation, and various adsorption techniques [10–13]. In adsorptive purification of wastewater from laundries of nuclear power plants, it is necessary to take into account that surfactants contained in such LRW can spontaneously form in solutions hydrophilic aggregates, micelles which contain up to 100 surfactant molecules. The state of surfactants in solution (as separate molecules, ions, or associates of these) and their sorbability depend on various factors: nature of surfactants, concentration and temperature of their solutions, etc. [10]. Adsorption is a commonly used method in water treatment and other separation processes. It is an attractive since it is a fast and simple operation besides the availability of a wide variety of commercial adsorbents [14]. The key factor for the adsorption process is the choice of adsorbent. A good quality adsorbent should have, fast kinetics of interaction with the adsorbate, porous structure resulting in high surface area and high adsorption capacity [15].

In our group, we used activated carbon prepared from Rice's straw, sawdust and commercial activated carbon in

the removal of radioisotopes such as cesium, europium and uranium in addition to nitrate and nitrite anions in single- and binary-component systems [14–18]. The objective of the present work is to examine the adsorptive removal of nonionic surfactant from wastewater and from low level liquid radioactive waste solutions. Triton X-100 (TX100) was chosen as model surfactants, because it is a commonly used non-ionic surfactant in the households as detergents or care products, soil remediation, immunochemistry and had a potential application foreground. Although the TX100 adsorption at the concentration below CMC (critical micelle concentration) has been studied, no studies are focused at concentration above CMC. The obtained results may be used as a starting point in waste water treatments.

Experimental

Reagents and chemicals

The model nonionic surfactant used in this study was polyoxyethylene glycol tertoctylphenyl ether (Triton X-100 or TX100) and obtained from Merck Chemicals. TX100 was used as received, without any further purification. Commercial available charcoal activated was supplied from *El Nasr Pharmaceutical Chemicals Company (Adwic)*, Egypt. All the reagents and chemicals used were of analytical reagent grade.

Instruments and apparatus

Surfactant analysis

After centrifugation, the concentration of TX100 in the clear supernatant was determined by measuring UV absorbance at 222 and 275 nm wavelength using UV–Vis spectrophotometer (Shimadzu, UV-1601 model). Quartz cells of 10 mm path length were used. A calibration plot (absorbance vs. concentration) was obtained by measuring absorbance of surfactant solution of known concentration.

Radioactive wastewater samples

In the case of radioactive waste, the metal ions in waste solution were determined radiometrically, using a high resolution (7.5 %) NaI(Tl) γ -ray spectrometry model 802-3X3 with pulse height multi-channel analyzer (McA), Canberra, USA.

Adsorbent characterization

Charcoal was characterized using analytical techniques such as: scanning electron microscope (SEM), energy-

dispersive X-ray spectroscopy (EDX), Fourier transform infrared (FT-IR), differential thermal analysis (DTA-TGA).

Fourier transform infrared spectrum was recorded using Nicolet is spectrometer from Meslo, USA to identify the functional groups using the KBr disc method. In this concern, the sample was thoroughly mixed with KBr as a matrix, the mixture was ground and then pressed with a special press to give a disc of standard diameter. The disk formed was examined in FTIR spectrophotometer in the range from 4,000 to 400 cm^{-1} .

Thermal stability of the adsorbent was studied with a Shimadzu DTG 60—thermal analyzer, Japan. It was used for the measurements of the phase changes and weight losses of the sample, respectively, at heating rate of 10 $^{\circ}\text{C}/\text{min}$ in presence of nitrogen gas to avoid thermal oxidation of the powder sample.

The surface morphology was determined with SEM and SEM-energy dispersive X-ray spectroscopy (EDX) using Jeol scanning electron microscope of JSM-6510A Model, Japan. The morphology and grain size of the particles were identified, operating with beams of primary electrons ranging from 5 to 30 keV. Samples were washed, dried and mounting on support and then made conductive with sputtered gold.

Surface area of charcoal was determined using nitrogen adsorption/desorption isotherm at 77 K on an automatic adsorption instrument (Quantachrome Instruments, Model Nova1000e series, USA) in relative pressure ranging from 10^{-6} to 0.999. Charcoal was degassed at 250 $^{\circ}\text{C}$ under nitrogen flow for 9 h. followed by their analysis to evaluate the porous parameters. The amount of nitrogen adsorbed onto the samples was used to calculate the specific surface area by means of the BET equation. The total pore volume (V_{pore}) was deduced from the adsorption data based on the manufacturer's software and the pore size distribution was derived from the Dubinin-Astakhov theory. The micropore volumes (V_{micro}) were deduced using the t-plot method.

For the equilibration experiments, the aqueous and solid phases were mixed together using a thermostated mechanical shaker of the type Julabo SW-20C. Germany, controlled within ± 1 $^{\circ}\text{C}$ and with stirring range from 20 to 2,000 rpm.

Adsorption experiments

An adsorption test on the charcoal was performed in order to determine the time needed to reach equilibrium and the pattern of the kinetics. For this purpose, samples of 0.05 g of charcoal were transferred into bottles containing 25 ml of surfactant solution. The bottles were shaken. The samples were taken from the shaker at 35 $^{\circ}\text{C}$ at predetermined

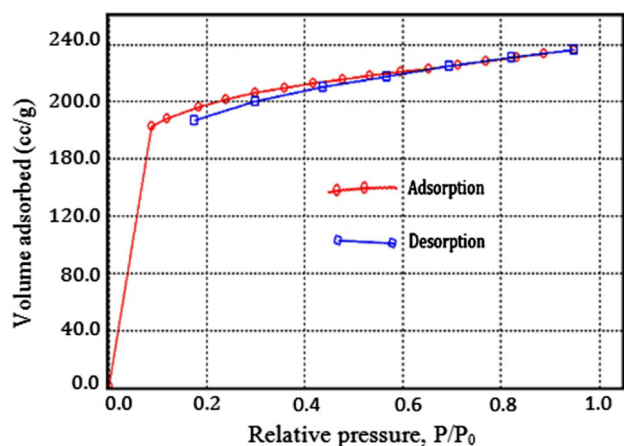


Fig. 2 Adsorption and desorption isotherm of N_2 by charcoal

time intervals. The residual concentration of surfactant at any time, t , was determined spectrophotometrically. All adsorption experimental tests were made twice. The percentage removal, $R\%$, of the surfactant at equilibrium and the amount of surfactant transferred onto the surface of charcoal at time t , q_t (mg/g) and at equilibrium q_e (mg/g), were calculated using the following relationships:

$$R\% = \frac{C_o - C_t}{C_o} \times 100 \quad (1)$$

$$q_t = (C_o - C_t) \frac{V}{m} \quad (2)$$

$$q_e = (C_o - C_e) \frac{V}{m} \quad (3)$$

where q_t shows the amount of surfactant adsorbed on charcoal at time t . C_o , C_t and C_e represent surfactant concentrations in the solution (mg/l) at initial, time t and equilibrium respectively. V is the volume of solution (L), and m is the mass of charcoal (g).

Results and discussion

Understanding of adsorption technique is possible with knowledge of the optimal conditions, which would show a better design and modeling process. Thus, the effect of some parameters like pH, contact time, mass of charcoal and initial concentration of surfactant on the uptake process was investigated. Adsorption studies were performed by batch technique to obtain the equilibrium data.

Adsorbent characterization

The shape of the adsorption isotherm can provide qualitative information on the adsorption process and the extent of the surface area available to the adsorbate. The properties

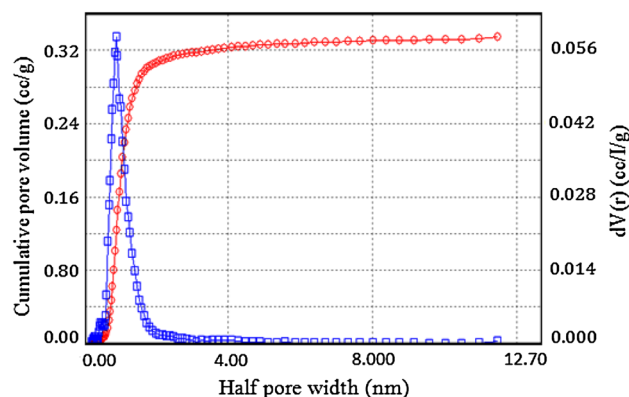


Fig. 3 Pore size distribution of charcoal

Table 1 Pore characteristic of charcoal sample

Parameter	Value
BET surface area (m^2/g)	610.99
Langmuir surface area (m^2/g)	946.74
Average pore radius (nm)	1.198
Total pore volume (cm^3/g)	0.366
Micropore volume (cm^3/g)	0.091
Mesopore volume (cm^3/g)	— ^a

^a This value not determined due to its low value

of the charcoal were characterized in terms of pore volume, surface area and pore size distribution. In order to determine specific surface area and porous volumes, charcoal was characterized by BET method. N_2 adsorption–desorption isotherms and pore size distribution analysis of charcoal are shown in Figs. 2 and 3.

The charcoal is a Type I according to the IUPAC isotherm, showing well-developed micropores. It is evident that most of the pore volume of the charcoal was filled below a relative pressure of about 0.1, indicating their high microporosity. After a sharp increase in the relative pressure to 0.1, the isotherms showed only very small increases in the pore volume, which is typical Type IV for mesopore volume. Type I exhibited by microporous solids and Type IV exhibited by mesoporous solids, initial part of the Type IV follows the same path as the Type II. The hysteresis loop of the sample is of H4 type. Type H4 loops feature both parallel and almost horizontal branches. This occurrence has been attributed to adsorption desorption in narrow slit-like pores.

The pore characteristic of charcoal is summarized in Table 1. The data obtained shows that charcoal offers high micropore volume. The data in this Table 1 also suggest that the mesopore volume of charcoal is negligible compared with micropore volume. It is defined that the size of micropore is less than 2 nm, that of mesopore is 2–50 nm,

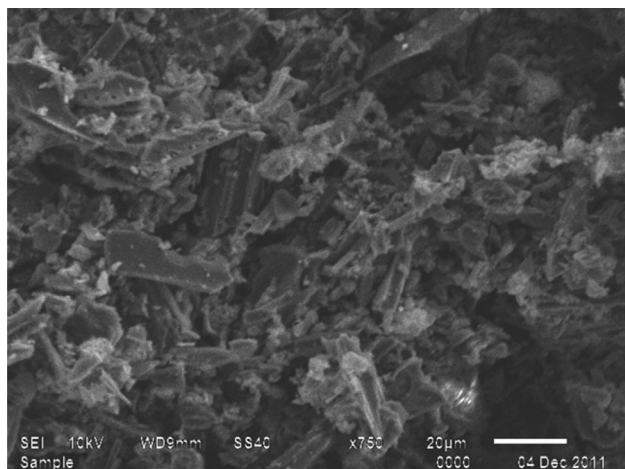


Fig. 4 SEM image of charcoal

and that of macropore is more than 50 nm. The pore size distribution seems located in the micropore region.

Studies on a charcoal's surface topography could provide important information on the degree of interaction between the charcoal particles and the TX100 surfactant molecules [19]. SEM was used to study the surface morphology of charcoal. The textural structure of the charcoal is presented as scanning electron micrograph at $\times 750$ magnification, Fig. 4. The SEM image showed the irregular texture and porous nature of the surface of the charcoal. The seemingly rough surface of the adsorbent is an indication of high surface area [19].

An FTIR spectrum of charcoal was obtained in the range of $4,000\text{--}400\text{ cm}^{-1}$. The spectrum of charcoal displays a number of absorption peaks, indicating the complex nature of the material under study, Fig. 5. A wide band with three maximum peaks can be noticed at $3,836$ and $3,739$ and $3,430\text{ cm}^{-1}$, are due to an O–H stretching mode of hydroxyl groups and adsorbed water, however, it must be indicated that the bands in that range have also been attributed to the hydrogen-bonded OH group of alcohols and phenols. The presence of –NH groups are also indicated by the band at $3,430\text{ cm}^{-1}$. Presences of $\text{C}\equiv\text{C}$ or $\text{C}\equiv\text{N}$ are indicated by the band at $2,356\text{ cm}^{-1}$ [20, 21]. The peak at $1,635\text{ cm}^{-1}$ is attributed to C=O amide that can be distinguished on surface of the charcoal as a result of the presence of ammonia and primary amines in the process of manufacturing of the sample. The peak occurring at $1,600\text{ cm}^{-1}$ is attributed to a vinyl-like C=C functional group or of carbonyl groups chelated to phenolic hydroxyl groups which support the above assumption [22]. Moreover, the band at $1,540\text{ cm}^{-1}$ is attributed to conjugated C=C or the aromatic ring. The peak occurring at $1,455\text{ cm}^{-1}$ is attributed to C–H bending vibrations. [23]. The peak at $1,159\text{ cm}^{-1}$ is ascribed to either Si–O or C–O

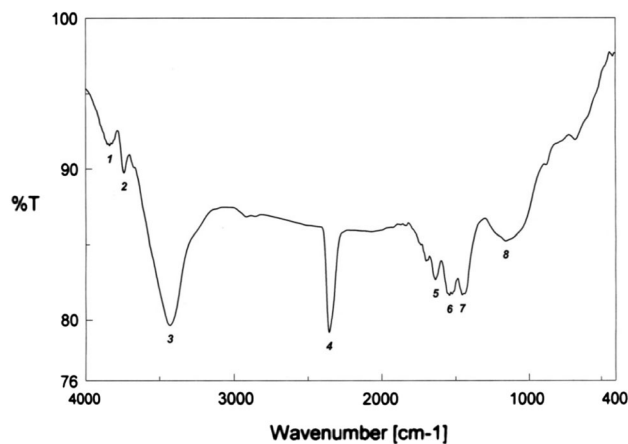


Fig. 5 FTIR spectrum of charcoal

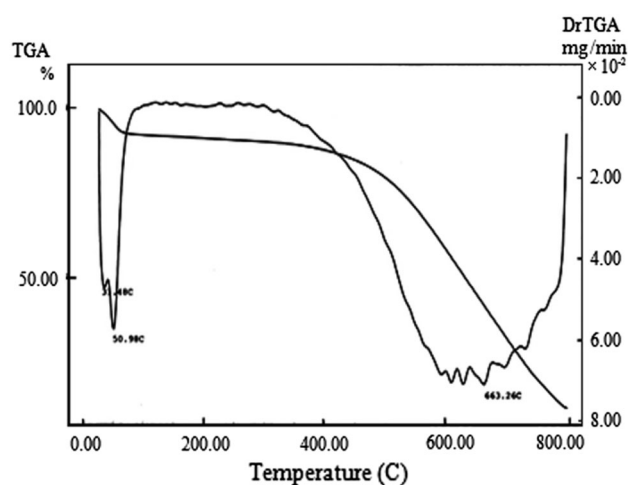


Fig. 6 TGA and DrTGA curves of charcoal

stretching in alcohol, ether or hydroxyl group [24] also can be associated with ether C–O symmetric and asymmetric stretching vibration (–C–O–C– ring) or attributed to the anti-symmetrical Si–O–Si stretching mode [25].

The thermal properties of charcoal were studied to investigate its thermal stability at high temperature operating condition. Thermogravimetric analysis, TGA, and differential thermal analysis, DTA, of charcoal sample up to $800\text{ }^{\circ}\text{C}$ are shown in Fig. 6. The sample has lost water content and light chemicals up to $100\text{ }^{\circ}\text{C}$ and exhibits no mass loss until about $400\text{ }^{\circ}\text{C}$. After $410\text{ }^{\circ}\text{C}$ mass loss rate has increased depending on the removal of volatiles organic components of sample and at $800\text{ }^{\circ}\text{C}$ total mass loss has reached to about 88 %. Disintegration of charcoal sample begins at $410\text{ }^{\circ}\text{C}$ and is ended at $790\text{ }^{\circ}\text{C}$. From the DTA curve, the first two endothermic peaks appear in the temperature range of $30\text{--}60\text{ }^{\circ}\text{C}$. Such endothermic effect corresponds to water release and light volatile organic

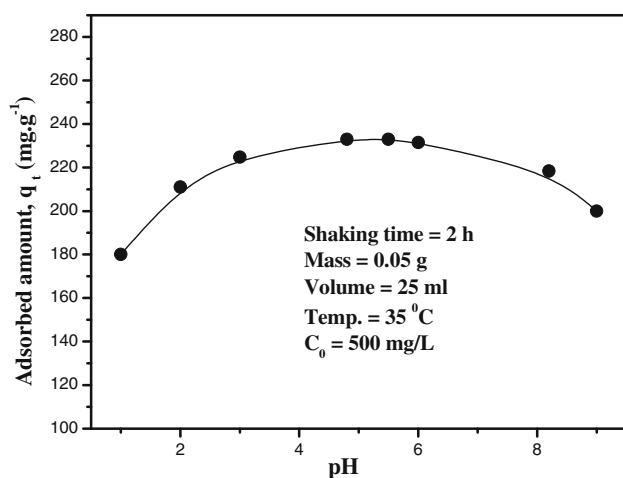


Fig. 7 Effect of initial pH solution on the adsorption of TX100 onto charcoal

compounds and the size of its area speaks about the amount of water and organic loss and temperature limits in which the release takes place. Other endothermic peaks appear in the temperature range of 600–780 °C.

Effect of pH on the adsorption process

The pH value of TX100 solutions plays an important role in the whole sorption process and particularly in capacity of charcoal as adsorbent. The pH of the solution affects the surface charge of the adsorbents as well as the degree of ionization of different pollutants. The H^+ and OH^- ions are adsorbed quite strongly and therefore the adsorption of other pollutants is affected by the solution pH. The change in pH affects the adsorptive process through dissociation of functional groups on the charcoal surface active sites. This subsequently leads to a shift in kinetics and equilibrium characteristics of adsorption process. To study the influence of pH on the adsorption capacity of charcoal to TX100, experiments were performed using different initial solution pH values, changing from 1 to 9. The results obtained are shown in Fig. 7.

Figure 7 shows that the effect of pH on the adsorption of TX100 is rather small. The charcoal exhibited high adsorption efficiency for TX100 with uptake higher than 220 mg/g within a pH range of 4.5–6.0, followed by a slight decrease with further increase in pH of solution. For this reason, a pH value of 5.0 was chosen for all further studies.

Effect of contact time and initial concentration on adsorption process

Sorption is time-dependent process and the equilibrium time is one of the most important parameters for

economical liquid waste treatment application. Short sorption equilibrium contact time favors the application of the sorption system. TX100 removal by charcoal was studied using three different initial concentrations so as to optimize the adsorption equilibrium time. Figure 8 illustrate the adsorption of TX100 on charcoal from aqueous solution as a function of contact time and initial concentration. It was found that the amount of TX100 adsorbed increases with increase in contact time, but after some time, it gradually approaches a constant value, denoting attainment of equilibrium. The uptake of TX100 by charcoal was very rapid at the beginning. The initial rapid phase may be due to the large number of vacant sites available at the initial period of the sorption. However, the amount of TX100 adsorbed increases with time and reaches a constant value after about 1 h. After the equilibrium time, the amount of TX100 adsorbed did not significant change with time. This plateau represents saturation of the active sites available on charcoal for interaction with TX100 molecules. It was assumed that the equilibrium time is that at which curves appear nearly asymptotic to the time axis. In the present case, the equilibrium time for TX100 removal was obtained at 60 min and hence considered for further study.

It can be seen that the adsorption of TX100 at different concentrations is rapid in the initial stages and gradually decreases with the progress of adsorption until the equilibrium is reached. The amount of TX100 adsorbed at equilibrium (q_e) increased from 230 to 270 mg/g as the concentration was increased from 500 to 700 mg/l. This may be because an increase in initial concentration enhances the interaction between TX100 molecules and the surface of charcoal. The initial concentration of TX100 provides an important driving force to overcome all mass transfer resistances of the TX100 between the aqueous and solid phases. Hence a higher initial concentration of surfactant will enhance the adsorption process. For higher initial concentration studied, it was found that there was no significant change on the equilibrium time at the observed initial TX100 concentration range. The uptake of TX100 surfactant versus time curves is smooth and continuous leading to saturation, suggesting the possibility of monolayer coverage of TX100 on the outer surface of charcoal.

Effect of adsorbent dosage

Adsorbent amount is an important parameter. It determines the capacity of an adsorbent for a given initial concentration of TX100 surfactant and helps to optimize a cost-effective dosage for a complete-mixed flow reactor. The effect of adsorbent dosage on TX100 removal was carried out with a wide range of 0.05–1.0 g and the results were presented in Fig. 9.

Fig. 8 Kinetic study for TX100 adsorption on charcoal at different concentrations

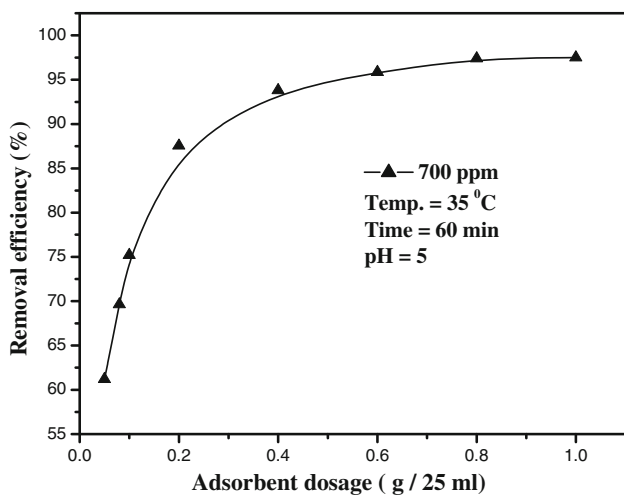
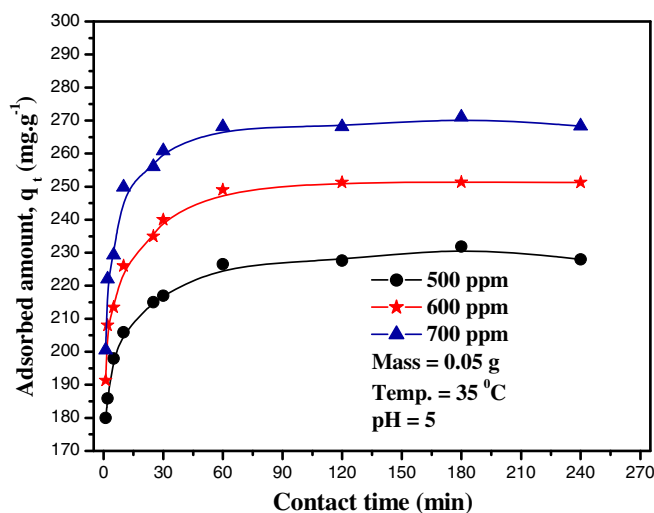


Fig. 9 Effect of adsorbent dose on TX100 removal

The observations reveal that an increase in the adsorption occurs with the corresponding increase in the amount of charcoal. The increase in the removal efficiency with simultaneous increase in charcoal dose is due to the increase in its surface area, and hence more active sites were available for the adsorption of TX100. The results showed that charcoal was efficient for 61.2 % removal of TX100 at the lowest dose of 0.05 g/25 ml and 97.5 % at maximum dose of 1 g/25 ml, respectively. At higher doses of charcoal, more sorbent surface area will be available for the sorption reaction and which results in higher removal.

It may also be observed that initially the removal of TX100 increases as the dose of charcoal is increased from 0.05 g till about 0.6 g/25 ml after which it increases slightly till 1.0 g/25 ml. This may be due to TX100 exhaustion, i.e. non-availability of TX100 or even due to non sorbability of TX100 as a result of charcoal-TX100 interaction.

Isotherm data analysis

At constant temperature, the relation between the amount of TX100 surfactant adsorbed and its concentration in the equilibrium solution is called adsorption isotherm. In adsorption, the TX100 adsorbate accumulates into the surface of charcoal which can be represented using adsorption isotherm models. Basically, adsorption isotherm is important to describe how TX100 interacts with adsorbents. Isotherms help in determining the feasibility of charcoal for treating TX100 in water [18]. Information derived from such data is important also in comparing different sorption media. In addition, analysis of the isotherm data is important to develop an equation which accurately represents the results and which could be used for design purposes and to optimize an operating procedure [19]. An attempt is made to test the Langmuir and Freundlich isotherms models for TX100 removal. The Langmuir and Freundlich isotherms are used most frequently to describe the adsorption data and for that reason, they were tested in this work [14].

Langmuir isotherm

The Langmuir conventional isotherm model is based on the assumption that (i) maximum adsorption corresponds to monolayer of TX100 adsorbate molecules on the homogeneous adsorbent surface, (ii) no interaction between the adsorbate and the adsorbent in the adsorption process, (iii) the energy of adsorption is constant for all molecules and (iv) there is no transmigration of adsorbate molecules in the plane of the surface. The linear form of Langmuir isotherm is illustrated in the following equation [19].

$$\frac{1}{q_e} = \frac{1}{Q} + \frac{1}{bQ} \left(\frac{1}{C_e} \right) \tag{4}$$

where C_e is the equilibrium concentration (mg/l), q_e is the amount of TX100 (mg/g) at equilibrium, Q is the theoretical monolayer capacity, and b is the sorption equilibrium constant related to the energy of adsorption. The linear plots of $1/C_e$ versus $1/q_e$ shows that adsorption obeys Langmuir adsorption model. A straight line was obtained with high correlation coefficient ($R^2 = 0.94$), confirming that Langmuir isotherm is applicable for adsorption of TX100 onto charcoal adsorbent. From the slope and intercept, one can determine the value of sorption equilibrium constant, b which gives a value of 0.0818 l/mg, and the monolayer capacity, Q of value of 285.71 mg/g.

One of the essential characteristics of Langmuir isotherm model can be expressed in terms of a dimensionless constant [19] called separation factor or equilibrium parameter, R_L , which can be calculated from Langmuir constant, b , as the following:

$$R_L = \frac{1}{1 + bC_0} \quad (5)$$

where b is a Langmuir constant and C_0 is the initial concentration of TX100. The value of R_L indicates the type of isotherm to be irreversible if, $R_L = 0$, favorable $0 < R_L < 1$, linear $R_L = 1$, or unfavorable $R_L > 1$. The R_L value was found to be equals 0.03 which is less than 1 and greater than 0 indicate favorable adsorption of TX100 onto charcoal.

Freundlich isotherm

The Freundlich isotherm equation was also applied to the adsorption of TX100 surfactant on charcoal. The Freundlich isotherm is commonly used to describe adsorption characteristics for heterogeneous adsorbent surface (multilayer adsorption). It generally agreed quite well compared to above model and experimental data over a moderate range of adsorbate concentrations. The logarithmic form of the Freundlich equation is [18]:

$$\log q_e = \log K + \frac{1}{n} \log C_e \quad (6)$$

where C_e is the equilibrium concentration (mg/l), n , K are constants which depend on the nature of the adsorbate, adsorbent and temperature. Plot of $\log q_e$ versus $\log C_e$ yielding a straight line indicates the confirmation of Freundlich isotherm model for sorption. The Freundlich constants $1/n$ and k can be determined from the slope and the intercept respectively, as illustrated in Table 2.

The constants K and n were found to be 139.96 and 7.89, respectively. The value of $1 < n < 10$ shows a favorable sorption of TX100 onto charcoal. The correlation coefficient for the Freundlich plot was found to be 0.96 indicating a better fit of the experimental data compared to

Table 2 Langmuir and Freundlich parameters for sorption of TX100 surfactant

Langmuir parameters				Freundlich parameters		
Q (mg/g)	R_L	b (L/mg)	R^2	K (mg/g)	n	R^2
285.71	0.03	0.055	0.94	139.96	7.89	0.96

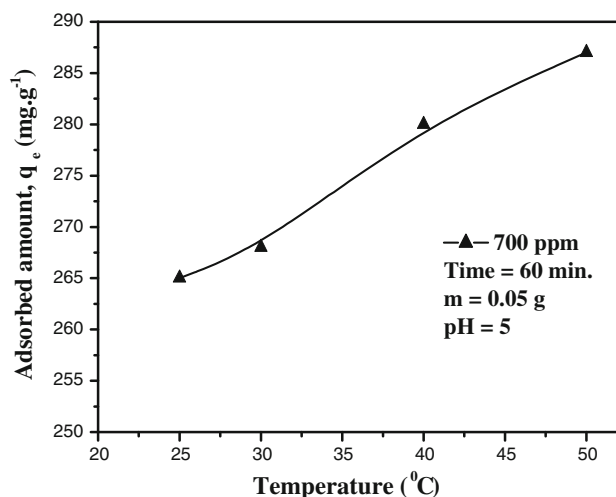


Fig. 10 Effect of temperature on the removal of TX100 onto charcoal

Langmuir plot. The adsorption of TX100 by charcoal obeys to Freundlich isotherm with high correlation coefficient (figures not shown, we took the results for the sake of brevity).

Effect of temperature and thermodynamic parameters

It is well known that temperature changes play an important role in sorption process [14, 15, 18]. To know an indication about thermodynamic of adsorption, effect of temperature on adsorption capacity should be studied. The plot of adsorption capacity of 700 μ g/ml as a function of temperature shows an increasing amount of adsorbed TX100 surfactant with temperature from 25 to 50 °C, indicating that the adsorption is an endothermic process, Fig. 10.

For TX100, the surface coverage increased at higher temperatures, this may be attributed to increased penetration of TX100 inside micropores at higher temperatures or the creation of new active sites or formation of more than one molecular layer on the surface of charcoal. The increase in the adsorption may be a result of increase in the mobility of TX100 molecules with increasing temperature. An increasing number of molecules may also acquire sufficient energy to undergo an interaction with active sites at

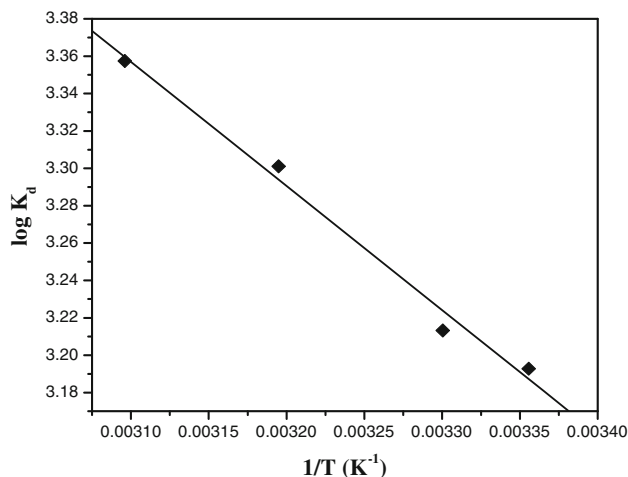


Fig. 11 Van't Hoff plot for adsorption of TX100

the surface of charcoal [26]. Furthermore, increasing temperature may produce a swelling effect within the internal structure of the charcoal which enabling large amount of TX100 to penetrate further [14]. The obtained results indicate that adsorption capacity of TX100 increased by increasing temperature.

The temperature dependence of the adsorption process is associated with changes in several thermodynamic parameters. Thermodynamic parameters such as Gibbs free energy, ΔG° , enthalpy, ΔH° , and entropy changes, ΔS° for the adsorption of TX100 onto charcoal can be calculated using Van't Hoff equation as the following [19, 27]:

$$\Delta G^\circ = -RT \ln K_d \tag{7}$$

$$\log \left(\frac{q_e}{C_e} \right) = \frac{\Delta S^\circ}{2.303R} + \frac{-\Delta H^\circ}{2.303RT} \tag{8}$$

$$\Delta G^\circ = \Delta H^\circ - T\Delta S^\circ \tag{9}$$

where K_d is the distribution coefficient; $K_d = q_e/C_e$ (L/g), R is the general gas constant ($R = 8.314$ J/mol K) and T is the absolute temperature (K). The relation between $\log K_d$ and $1/T$ is given in Fig. 11. This figure showed a linear relation ($R^2 = 0.98$), the values of enthalpy change and entropy change can be calculated from the slope and intercept, respectively. Values of these parameters are listed in Table 3.

From these values one can conclude that the positive value of ΔH° confirming the endothermic nature of the adsorption process. This phenomenon may be due to the behavior of TX100 in aqueous solution, which displaced more than single water molecule adsorbed previously on charcoal which leads to endothermic adsorption process. In addition the small values of ΔH° (12.72 kJ/mol) are not compatible with the formation of strong chemical bonds between TX100 molecules and the sites on the charcoal

Table 3 Thermodynamic parameters for adsorption of TX100 onto charcoal

Temp. K	K_d L/g	ΔH° (KJ/mol)	ΔS° (J/mol K)	ΔG° (KJ/mol)
298	1.559	12.72	103.69	-18.19
303	1.634			-18.70
313	2.00			-19.74
323	2.278			-20.78

surface [27]. The positive value of ΔS° shows the increased randomness at the charcoal/solution interface with some structural changes in the charcoal and an affinity of charcoal toward TX100 [19]. The obtained negative value of free energy change, ΔG° , confirming that adsorption of TX100 onto charcoal is spontaneous and thermodynamically favorable process [28].

Mechanism of TX100 adsorption

There are several mechanisms by which surfactant molecules may adsorb onto the solid phase adsorbents from aqueous media. Generally, the adsorption of surfactants involves single molecules adsorption rather than micelles adsorption [29]. i. *Ion exchange*: replacement of counter ions adsorbed onto the substrate from the solution by similarly charged surfactant molecules. ii. *Ion pairing*: adsorption of surfactant from aqueous medium onto oppositely charged sites unoccupied by counter ions. iii. *Hydrophobic bonding*: adsorption occurs by this mechanism when there is an attraction between a hydrophobic group of adsorbed molecule and a molecule present in the aqueous media. iv. *Adsorption by polarization of π electrons*: when the surfactant contains electron-rich aromatic nuclei; the adsorbent has strongly positive sites, attraction between electron rich aromatic ring of the adsorbate and positive sites on the solid phase adsorbent results in adsorption. v. *Adsorption by dispersion forces*: Adsorption by London–van der Waals force between adsorbate and solid phase adsorbent increases with the increasing molecular weight of the adsorbate molecule.

Comparison of adsorption capacities of various adsorbents for TX100 surfactant

Table 4 represents a comparison of the adsorption capacity of charcoal obtained in this study with other adsorbents obtained in the literature for the adsorption of TX100. It shows that charcoal can be considered as a promising material for removing TX100, even compared to some other low cost adsorbents and activated carbons previously suggested for the uptake of TX100 from aqueous solutions.

Table 4 Comparison of q_{\max} for various adsorbents

Adsorbent	q_{\max} (mg/g)	References
Granitic sand	1.47×10^{-4}	[30]
Soil	0.012	[31]
Humin	4.38	[32]
Humic acid	26.30	[32]
Soil	110.0	[32]
Activated carbon ^a	150.00	[33]
Activated carbon ^a	230.00	[33]
Activated carbon ^a	246.20	[34]
Activated carbon ^a	298.93	[34]
Activated carbon ^a	300.00	[33]
Activated carbon ^a	332.84	[34]
Commercial charcoal	285.71	This work

^a Activated carbon with different modifications

Table 5 Removal of TX100 surfactant from real wastewater and synthetic samples

Sample ^a	Sample composition, ($\mu\text{g/ml}$) or M or (count/s)	Removal (%)
Radioactive wastewater ^b	$^{60}\text{Co} = 31.20$ $^{134}\text{Cs} = 954.34$	98.30
Radioactive wastewater ^c	$^{60}\text{Co} = 22.33$ $^{134}\text{Cs} = 663.30$	97.60
Tap water	–	97.00
Synthetic sample	$\text{NaNO}_3 = 0.8 \text{ M}$ $\text{EDTA} = 10 \mu\text{g/ml}$ $\text{Co(II)} = 2 \mu\text{g/ml}$	98.40

EDTA ethylenediaminetetraacetic acid

^a All samples spiked with 300 $\mu\text{g/ml}$ TX100

^{b,c} Radioactive wastewater samples from wastewater treatment plant

Application to real samples

One of the most important factors that should be considered when testing any solid phase used as adsorbent in the removal of any pollutant(s) is the application to real samples. In this study, two different real radioactive wastewater samples were collected from Wastewater Treatment Plant. To verify the applicability of the charcoal for the adsorptive removal of surfactant from real wastewater samples, the samples were therefore spiked with TX100 (spiking with 300 $\mu\text{g/ml}$) after characterization of these radioactive samples.

Under the optimal conditions, the treatment of tap water polluted with surfactant and synthetic sample containing mineral salts and complexing agent was investigated in order to examine the matrix effect on the treatment process. Adsorption experiments using charcoal as adsorbent was then performed, Table 5.

The results obtained showed that the removal efficiencies of TX100 surfactant are about 98 %. The results also indicated that charcoal is a good adsorbent for the removal of surfactant from surfactant-containing wastewaters and confirmed the validity of the proposed method for real samples. The attractive features of charcoal are that it is commercially available, effective and of low-cost.

Conclusions

Direct and indirect releases of large quantities of surfactants to the environment may result in serious health and environmental problems. Therefore, surfactants should be removed from water before release to the environment or delivery for public use. In nuclear power plants, laundry waste water is generated, in which such organic compounds as surfactants are included. Batch adsorption studies for the removal of TX100 from aqueous solutions have been carried out using commercial charcoal. The adsorption isotherm studies showed that Freundlich adsorption isotherm model adequately described the adsorption of TX100 onto charcoal. The thermodynamic parameters showed a chemically favored, spontaneous and endothermic adsorption. The present study concludes that commercial charcoal used under these conditions, has a considerable potential as an effective sorbent for the removal of TX100 surfactant from wastewater and radioactive wastewater. It can therefore have a place in the treatment of surfactant from wastewater and radioactive wastewater since it is of a low-cost and commercially available adsorbent.

Acknowledgments The author would like to express their deep thanks to prof. Dr. Sohair A. El-Reefy for her valuable support and review this text. The author is thankful to Prof. Dr. M. A. Hilal for her kind help and valuable support during the experimental section of this work.

References

1. Suarez L, Diez MA, Garcia R, Riera FA (2012) J Ind Eng Chem 18:1859–1873
2. Shen D, Wang F, Kang Q, Yang D (2004) Sens Trans Mag 40:152–161
3. Mimanne G, Sennour R, Benghalm A, Taleb S, Benhab K (2012) J Mater Environ 3:712–725
4. Bhagyashree K, Kar A, Kasar S, Kumar S, Shukla R, Mishra RK, Kaushik CP, Tyagi AK, Tomar BS (2014) J Radioanal Nucl Chem 299:1433–1437
5. Younjin P, Young L, Won SS, Sang-June C (2010) Chem Eng 162:685–695
6. Toshiaki M, Takashi N (2000) Carbon 38:709–714
7. Dulama M, Deneanu N, Pavelescu M, Pasăre L (2009) Rom J Phys 54:851–859
8. Park Y, Lee Y, Shin WS, Choi S (2010) Chem Eng J 162:685–695

9. Guerrero A, Gosi S, Allegro VR (2009) *J Hazard Mater* 161:1250–1254
10. Ivanets MG, Savitskaya TA, Grinshpan D, Tsygankova NG, Savkin A (2012) *Russ J Appl Chem* 85:46–51
11. Nishi T, Matsuo T (2001) WM'01 conference, February 25–March 1, Tucson, AZ
12. Beltrn J, Snchez J, Barrado M (2012) *Chem Eng J* 180:128–136
13. Yong Eng Y, Sharma VK, Ray AK (2012) *Sep Purif Technol* 92:43–49
14. Attallah MF, Ahmed IM, Hamed MM (2013) *Environ Sci Pollut Res* 20:1106–1116
15. El-Sayed AA, Hamed MM, Hammad H, El-Reefy SA (2007) *Radiochim Acta* 95:43–48
16. Hassan HS, Attallah MF, Yakout SM (2010) *J Radioanal Nucl Chem* 286:17–26
17. Hamed MM, Ahmed IM, Metwally SS (2013) *J Ind Eng Chem* 20:2370–2377
18. Hamed MM, Yakout SM, Hassan HS (2013) *J Radioanal Nucl Chem* 295:697–708
19. Abbas M, Kaddour S, Trari M (2014) *J Ind Eng Chem* 20:745–751
20. Yang T, Lua A (2003) *J Colloid Interface Sci* 267:408–417
21. Singh SR, Singh AP (2012) *Int J Environ Res* 6:917–924
22. Mattson JS, Mark HB Jr (1969) *J Colloid Interface Sci* 31:131–144
23. Park SH, McClain S, Tian ZR, Suib SL, Karwacki C (1997) *Chem Mater* 9:176–183
24. Attia AA, Rashwan WE, Khedr SA (2006) *Dyes Pigment* 69:128–136
25. Lapuente R, Cases F, Garcés P, Morallón E, Vázquez JL (1998) *J Electroanal Chem* 451:163–171
26. Bouhamed F, Elouear Z, Bouzid J, Ouddane B (2013) *Desalin Water Treat* 22:1–11
27. Milojkovic JV, Milojkovic ML, Stojanovic MD, Lopovic ZR, Petrovic MC, Sostaric TD, Ristic MD (2014) *J Chem Technol Biotechnol* 89:662–670
28. Kyzas GZ, Deliyanni EA, Matis KA (2014) *J Chem Technol Biotechnol* 89:196–205
29. Paria S, Khilar KC (2004) *Adv Colloid Interface Sci* 110:75–95
30. Khan MN, Zareen U (2004) *J Iran Chem Soc* 1:152–158
31. Liu Z, Edwards DA, Luthy R (1992) *Water Res* 26:1337–1345
32. Guangzhi Z, Hao HU, Weiling S, Jinren N (2009) *J Environ Sci* 21:795–800
33. Ahn CK, Kim YM, Woo SH, Park JM (2007) *Chemosphere* 69:1681–1688
34. Gonzalez CM, Gonzalez ML, Gomez V, Bruque JM, Labajos BL (2001) *Carbon* 39:849–855